

Numerical simulation of SARS-CoV-2 by SKAZI scheme

Sadaqat Ali ¹

Abstract

In this paper, we present the mathematical model for severe acute respiratory syndrome coronavirus 2 (SARS-CoV-2). The outbreak of SARS-CoV-2 has led to 2,192,469 confirmed cases as of April 17, 2020 and total deaths are 147,360 in 210 different countries, area or territories. The basic reproductive number is formulated using next generation approach. The sensitivity analysis of reproductive number and local stability analysis of mathematical model are discussed. Also, we present numerical approximations for the disease free and endemic equilibrium points for infection of SARS-CoV-2. Also, we propose an efficient SKAZI scheme. Lastly, we present numerical experimentation of SKAZI scheme. The disease free and endemic equilibrium points are graphical reveal for stability and instability of mathematical model.

Key words. SARS-CoV-2, Mathematical model, Reproductive number, Equilibria, Sensitivity analysis, Uncertainty level, Consistent.

AMS subject classifications. 92B05, 93D20, 65N12

1 Introduction

The SARS-CoV-2 encloses to a family of viruses which probably show numerous symptoms for example fever, pneumonia, lung infection and breathing difficulty [1]. The WHO officially declared the 2019 novel coronavirus as coronavirus disease (COVID-19). The WHO established that the epidemic of the SARS-CoV-2 was related with Seafood Marketplace of the Huanan South China [11], but no specific animal was identified. After that researchers and scientists instantly started to investigate the source of the SARS-CoV-2, and the first genome of COVID-19 was investigated by Prof. Yong-Zhen Zhang, on 10 January 2020 [8]. SARS-CoV-2 has now been confirmed as a Public Health Emergency of International Concern by the WHO [7]. By recent research, early cases are exposed by contact direct belongs to original seafood market [4, 10]. After that, a secondary source of infection of SARS-CoV-2 was transmitted by close contact [3].

The emergence and transmission of a SARS-CoV-2 from Wuhan, China, has turned out to be a worldwide health concern. Unfortunately, the recognition of the SARS-CoV-2

¹*Co-responding Author:* Department of mathematics and statistics, The University of Lahore, Gujrat Campus, 50700 Gujrat, Pujnab, Pakistan, *email:* sadaqateshu@gmail.com

in late December 2019, numerous countries have reported random imported cases in the midst of travelers returning from China. The epidemic was first acknowledged in Wuhan, China, in December, 2019, with untimely cases being accounted in the city. Most globally exported cases reported to date have history of travel to Wuhan. Initially steps of a new contagious disease is epidemic. It is essential to comprehend the transmission dynamics of the infection. Approximation of modifications in transmission of SARS-CoV-2 along with time can supply imminent into the epidemiological condition and recognize whether epidemic control procedures are having a quantifiable outcome. It can report to prediction regarding potential future growth, help out guesstimate menace to other countries, and lead us to design of substitute interventions.

A respiratory pathogen of fairly high virulence from a virus cluster that has an strange ability of emerging species restrictions in a major population center and travel core shortly prior to the largest travel period of the year **the Chinese Spring festival**. Early genomic evaluation exposed for the most part directly associated viruses to SARS-CoV-2 came from bats [4].

For numeric solution, there is no exact formula to compute the analytic solution of ordinary differential equation which could be either linear or non-linear. The equilibrium point both disease free and endemic, are approximated by SKAZI scheme. When the SKAZI scheme converges, the numerical solution converges to equilibrium point of the iteration. Also, SKAZI scheme is guarantee convergence to the exact solution along with optimal minimum percentage error.

1.1 Overview of the article

Section 2 gives the basic framework and mathematical model for proposed epidemiological model of infection SARS-CoV-2. The proposed model (1) is a non-linear system of first order ordinary differential equations. The qualitative analysis for disease free and endemic equilibrium points and local stability analysis are analyzed in (Theorem 2.1). The basic reproductive number is formulated and sensitivity analysis is presented.

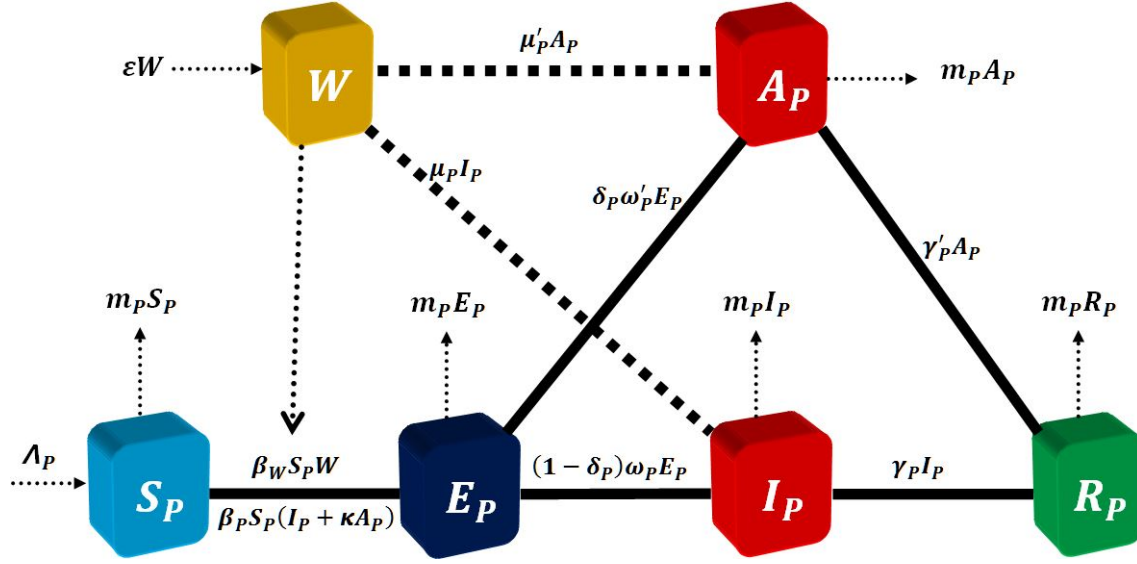
In section 3, the SKAZI scheme along with uncertainty level Ψ is introduced. The bounds of global error of SKAZI scheme in terms of truncation error is analyzed (Theorem 3.1). The convergence of SKAZI scheme is analyzed (Theorem 3.2) by means of consistency condition relative minimization of truncation error. The discrete transformation of purposed model (1) is formulated.

Finally, in section 4, we present the numerical simulation computed by SKAZI scheme.

2 Mathematical model of SARS-CoV-2

The schematic model for the Reservoir-People (RP) SARS-CoV-2 transmission network model is presented in Figure 1. The presenting model is highly non-linear bio-mathematical model [2].

Figure 1: Dynamic illustration of SARS-CoV-2 model.



The state variable and associated parameter for this model is given in Table 1 and Table 2.

Table 1: The state variables of SAR-CoV2 infection model.

| Symbol | Denoted by |
|----------|--|
| $S_P(t)$ | Susceptible people |
| $E_P(t)$ | Exposed people |
| $I_P(t)$ | Symptomatic infected people |
| $A_P(t)$ | Asymptomatic infected people |
| $R_P(t)$ | Removed people |
| $W(t)$ | SARS-CoV-2 in reservoir (the seafood market) |

Based on the flow chart of transmission of SARS-CoV2 infection in human population

as depicted in figure 1, we have the following system of equations:

$$\begin{aligned}
\frac{dS_P}{dt} &= \Lambda_P - \beta_P S_P (\kappa A_P + I_P) - m_P S_P - \beta_W W S_P \\
\frac{dE_P}{dt} &= \beta_P S_P (\kappa A_P + I_P) - E_P m_P - E_P (1 - \delta_P) \omega_P - E_P \delta_P \omega'_P + W S_P \beta_W \\
\frac{dI_P}{dt} &= E_P (1 - \delta_P) \omega_P - I_P (m_P + \gamma_P) \\
\frac{dA_P}{dt} &= E_P \delta_P \omega'_P - A_P (m_P + \gamma'_P) \\
\frac{dR_P}{dt} &= A_P \gamma'_P + I_P \gamma_P - m_P R_P \\
\frac{dW}{dt} &= A_P \mu'_P + I_P \mu_P - \varepsilon W
\end{aligned} \tag{1}$$

The feasible region of model (1) is $\Omega = \{(S_P, E_P, I_P, A_P, R_P, W) \in \mathbb{R}_+^6 : N \leq \frac{\Lambda_P}{m_P}\}$, where $N(t) = S_P(t) + E_P(t) + I_P(t) + A_P(t) + R_P(t) + W(t)$.

2.1 Equiliria and stability analysis

The mathematical model (1) have following equilibrium points,

- Disease free equilibrium points $E^0 = (S_P^0, 0, 0, 0, 0, 0)$, where

$$S_P^0 = \frac{\Lambda_P}{m_P}$$

- The endemic equilibrium points $E^* = (S_P^*, E_P^*, I_P^*, A_P^*, R_P^*, W^*)$,

$$\begin{aligned}
S_P^* &= -\frac{c\varepsilon c' (m_P + \delta_P \omega'_P - (\delta_P - 1) \omega_P)}{c' (\delta_P - 1) \omega_P (\varepsilon \beta_P + \mu_P \beta_W) - c \delta_P \omega'_P (\varepsilon \kappa \beta_P + \beta_W \mu'_P)} \\
E_P^* &= \frac{c \delta_P \omega'_P (\varepsilon c' m_P - \Lambda_P (\varepsilon \kappa \beta_P + \beta_W \mu'_P)) + c' (c \varepsilon m_P - (\delta_P - 1) \omega_P (c \varepsilon m_P - \Lambda_P (\varepsilon \beta_P + \mu_P \beta_W)))}{(m_P + \delta_P \omega'_P - (\delta_P - 1) \omega_P) (c' (\delta_P - 1) \omega_P (\varepsilon \beta_P + \mu_P \beta_W) - c \delta_P \omega'_P (\varepsilon \kappa \beta_P + \beta_W \mu'_P))} \\
I_P^* &= -\frac{\varepsilon c' m_P (\delta_P - 1) \omega_P}{c' (\delta_P - 1) \omega_P (\varepsilon \beta_P + \mu_P \beta_W) - c \delta_P \omega'_P (\varepsilon \kappa \beta_P + \beta_W \mu'_P)} - \frac{(\delta_P - 1) \Lambda_P \omega_P}{c (m_P + \delta_P \omega'_P - \delta_P \omega_P + \omega_P)} \\
A_P^* &= \frac{\delta_P \omega'_P (c \delta_P \omega'_P (\varepsilon c' m_P - \Lambda_P (\varepsilon \kappa \beta_P + \beta_W \mu'_P)) + c' (c \varepsilon m_P^2 - (\delta_P - 1) \omega_P (c \varepsilon m_P - \Lambda_P (\varepsilon \beta_P + \mu_P \beta_W))))}{c' (m_P + \delta_P \omega'_P - (\delta_P - 1) \omega_P) (c' (\delta_P - 1) \omega_P (\varepsilon \beta_P + \mu_P \beta_W) - c \delta_P \omega'_P (\varepsilon \kappa \beta_P + \beta_W \mu'_P))} \\
R_P^* &= -\frac{B (c \delta_P \omega'_P (\varepsilon c' m_P - \Lambda_P (\varepsilon \kappa \beta_P + \beta_W \mu'_P)) + c' (c \varepsilon m_P^2 - (\delta_P - 1) \omega_P (c \varepsilon m_P - \Lambda_P (\varepsilon \beta_P + \mu_P \beta_W))))}{c c' m_P (m_P - (\delta_P - 1) \omega_P + \delta_P \omega'_P) (c' (\delta_P - 1) \omega_P (\varepsilon \beta_P + \mu_P \beta_W) - c \delta_P \omega'_P (\varepsilon \kappa \beta_P + \mu'_P \beta_W))} \\
W^* &= -\frac{D (c \delta_P \omega'_P (\varepsilon c' m_P - \Lambda_P (\varepsilon \kappa \beta_P + \beta_W \mu'_P)) + c' (c \varepsilon m_P^2 - (\delta_P - 1) \omega_P (c \varepsilon m_P - \Lambda_P (\varepsilon \beta_P + \mu_P \beta_W))))}{c \varepsilon c' (m_P + \delta_P \omega'_P - (\delta_P - 1) \omega_P) (c' (\delta_P - 1) \omega_P (\varepsilon \beta_P + \mu_P \beta_W) - c \delta_P \omega'_P (\varepsilon \kappa \beta_P + \beta_W \mu'_P))}
\end{aligned} \tag{2}$$

where $B = c' \gamma_P (\delta_P - 1) \omega_P - c \delta_P \gamma'_P \omega'_P$, $D = c' (\delta_P - 1) \mu_P \omega_P - c \delta_P \mu'_P \omega'_P$, $c = m_P + \gamma_P$ and $c' = m_P + \gamma'_P$. The reproductive number \mathbb{R}_0 is evaluated by next generation approach [5] along with following Jacobian matrix J_0 (for disease free equilibrium E_0) with infection matrices F and rest of transmission matrix V .

$$J_0 = \begin{pmatrix} -m_P & 0 & -\frac{\beta_P \Lambda_P}{m_P} & -\frac{\kappa \beta_P \Lambda_P}{m_P} & 0 & -\frac{\beta_W \Lambda_P}{m_P} \\ 0 & -m_P + (\delta_P - 1) \omega_P - \delta_P \omega_P & \frac{\beta_P \Lambda_P}{m_P} & \frac{\kappa \beta_P \Lambda_P}{m_P} & 0 & \frac{\beta_W \Lambda_P}{m_P} \\ 0 & -(\delta_P - 1) \omega_P & -m_P - \gamma_P & 0 & 0 & 0 \\ 0 & \delta_P \omega_P & 0 & -m_P - \gamma'_P & 0 & 0 \\ 0 & 0 & \gamma_P & \gamma'_P & -m_P & 0 \\ 0 & 0 & \mu_P & \mu'_P & 0 & -\varepsilon \end{pmatrix}, \quad (3)$$

$$V = \begin{pmatrix} m_P & 0 & 0 & 0 & 0 & 0 \\ 0 & m_P - (\delta_P - 1) \omega_P + \delta_P \omega_P & 0 & 0 & 0 & 0 \\ 0 & -(1 - \delta_P) \omega_P & m_P + \gamma_P & 0 & 0 & 0 \\ 0 & -\delta_P \omega_P & 0 & m_P + \gamma'_P & 0 & 0 \\ 0 & 0 & -\gamma_P & -\gamma'_P & m_P & 0 \\ 0 & 0 & -\mu_P & -\mu'_P & 0 & \varepsilon \end{pmatrix}. \quad (4)$$

And

$$F = \begin{pmatrix} 0 & 0 & -\frac{\beta_P \Lambda_P}{m_P} & -\frac{\kappa \beta_P \Lambda_P}{m_P} & 0 & -\frac{\beta_W \Lambda_P}{m_P} \\ 0 & 0 & \frac{\beta_P \Lambda_P}{m_P} & \frac{\kappa \beta_P \Lambda_P}{m_P} & 0 & \frac{\beta_W \Lambda_P}{m_P} \\ 0 & 0 & 0 & 0 & 0 & 0 \\ 0 & 0 & 0 & 0 & 0 & 0 \\ 0 & 0 & 0 & 0 & 0 & 0 \\ 0 & 0 & 0 & 0 & 0 & 0 \end{pmatrix}. \quad (5)$$

The basic reproductive number is the spectral radius of matrix FV^{-1} that is, $\rho(FV^{-1})$ and given as,

$$\begin{aligned} \mathbb{R}_0 = & \frac{\beta_P \Lambda_P \omega_P (\varepsilon m_P ((\kappa - 1) \delta_P + 1) + \varepsilon (\kappa \gamma_P \delta_P - \delta_P \gamma'_P + \gamma'_P))}{\varepsilon m_P (m_P + \gamma_P) (m_P + \omega_P) (m_P + \gamma'_P)} \\ & + \frac{\Lambda_P \omega_P \beta_W (m_P (\delta_P \mu'_P - \delta_P \mu_P + \mu_P) + (\delta_P - 1) \mu_P (-\gamma'_P) + \gamma_P \delta_P \mu'_P)}{\varepsilon m_P (m_P + \gamma_P) (m_P + \omega_P) (m_P + \gamma'_P)} \end{aligned} \quad (6)$$

Theorem 2.1 For disease free equilibrium E_0 the system (1) is locally asymptotically stable if $\text{Re}(\lambda_i) < 0$ and unstable if $\text{Re}(\lambda_i) > 0$ for $i = 1, 2, \dots, 6$.

Proof: Let the system (1) holds for disease free equilibrium E_0 and J_0 be the Jacobian

matrix of system (1),

$$J_0 = \begin{pmatrix} -m_P & 0 & -\frac{\beta_P \Lambda_P}{m_P} & -\frac{\kappa \beta_P \Lambda_P}{m_P} & 0 & -\frac{\beta_W \Lambda_P}{m_P} \\ 0 & -m_P + (\delta_P - 1) \omega_P - \delta_P \omega_P & \frac{\beta_P \Lambda_P}{m_P} & \frac{\kappa \beta_P \Lambda_P}{m_P} & 0 & \frac{\beta_W \Lambda_P}{m_P} \\ 0 & -(\delta_P - 1) \omega_P & -m_P - \gamma_P & 0 & 0 & 0 \\ 0 & \delta_P \omega_P & 0 & -m_P - \gamma'_P & 0 & 0 \\ 0 & 0 & \gamma_P & \gamma'_P & -m_P & 0 \\ 0 & 0 & \mu_P & \mu'_P & 0 & -\varepsilon \end{pmatrix}, \quad (7)$$

Then the eigenvalues of Jacobian matrix J_0 (7) along with the numerical values of parameters given in Table 2 are given as follows,

$$\begin{aligned} \lambda_1 &= -0.351549 < 0, & \lambda_2 &= -0.190414 < 0, & \lambda_3 &= -0.100507 < 0, \\ \lambda_4 &= -0.048658 < 0, & \lambda_5 &= -0.018 < 0, & \lambda_6 &= -0.018 < 0. \end{aligned}$$

All of the eigenvalues λ_i of Jacobian matrix J_0 have strictly negative, that is, $Re(\lambda_i) < 0$ for all $i = 1 : 6$. This completes the proof.

Theorem 2.2 Suppose that the mathematical model (1) consists of all feasible solutions along with non-negative initial result then it remains non-negative for all time t .

Proof: Let the mathematical model (1) satisfy the initial non-negative solution, i.e.,

$$S_P(0) \geq 0, \quad E_P(0) \geq 0, \quad I_P(0) \geq 0, \quad A_P(0) \geq 0, \quad R_P(0) \geq 0, \quad W(0) \geq 0.$$

The rest of principal condition can be computed as follows,

$$\frac{S_P}{dt} = \Lambda_P - DS_P \quad (8)$$

where $D = \beta_P (\kappa A_P + I_P) + m_P + W (\beta_W)$, while the solution of variable S_P can be computed by following result,

$$S_P = S_P(0)e^G + \int_0^t \pi e^{H(u)} du \geq 0 \quad (9)$$

where $G = -\int_0^t G(u) du$ and $H(u) = -\int_0^t G(\omega) d\omega$. This gives the non-negativity of $S_P(0)$, that is $S_P(0) \geq 0$ for all time $t \geq 0$ respectively. The non-negativity of rest variables in the system (1) is presented as follows,

$$\begin{aligned} \frac{dE_P}{dt} &= \beta_P S_P (\kappa A_P + I_P) - E_P m_P - E_P (1 - \delta_P) \omega_P - E_P \delta_P \omega'_P + W S_P \beta_W \\ \frac{dI_P}{dt} &= E_P (1 - \delta_P) \omega_P - I_P (m_P + \gamma_P) \\ \frac{dA_P}{dt} &= E_P \delta_P \omega'_P - A_P (m_P + \gamma'_P) \\ \frac{dR_P}{dt} &= A_P \gamma'_P + I_P \gamma_P - m_P R_P \\ \frac{dW}{dt} &= A_P \mu'_P + I_P \mu_P - \varepsilon W \end{aligned} \quad (10)$$

In term of matrix demonstration, the above system can be expressed as follows,

$$\frac{dF(t)}{dt} = H(t) + MF(t) \quad (11)$$

where,

$$F(t) = \begin{pmatrix} E_P(t) \\ I_P(t) \\ A_P(t) \\ R_P \\ W \end{pmatrix}, \quad H(t) = \begin{pmatrix} 0 \\ m_P + \gamma_p \\ m_P + \gamma'_p \\ 0 \\ 0 \end{pmatrix} \quad (12)$$

$$M = \begin{pmatrix} -m_P + (\delta_P - 1)\omega_P - \delta_P\omega_{P1} & \frac{\beta_P\Lambda_P}{m_P} & \frac{\kappa\beta_P\Lambda_P}{m_P} & 0 & \frac{\beta_W\Lambda_P}{m_P} \\ (1 - \delta_P)\omega_P & -m_P - \gamma_P & 0 & 0 & 0 \\ \delta_P\omega_{P1} & 0 & -m_P - \gamma_{P1} & 0 & 0 \\ 0 & \gamma_P & \gamma_{P1} & -m_P & 0 \\ 0 & \mu_P & \mu_{P1} & 0 & -\varepsilon \end{pmatrix} \quad (13)$$

$$= \begin{pmatrix} -0.2103 & 0.1215 & 0.0607 & 0 & 0.2835 \\ 0.1826 & -0.1904 & 0 & 0 & 0 \\ 0.0096 & 0 & -0.1904 & 0 & 0 \\ 0 & 0.1724 & 0.1724 & -0.018 & 0 \\ 0 & 0.0001 & 0.0005 & 0 & -0.1 \end{pmatrix}$$

The matrix M is Matzler matrix and therefore, the by result presented in [6], the mathematical model (1) is monotone. This pridict us to the fact that R_+^5 is invariant with respect to stream of the model (1). This completes the proof.

2.2 \mathbb{R}_0 -sensitivity analysis

The sensitivity analysis of reproductive numbers \mathbb{R}_0 is analyzed by taking partial derivative with respect to each parameter. These partial differentiation of \mathbb{R}_0 with respect to parameters are computed as follows,

$$\begin{aligned} \frac{\partial \mathbb{R}_0}{\partial \Lambda_P} &= \frac{\beta_P \omega_P (\varepsilon m_P ((\kappa - 1)\delta_P + 1) + \varepsilon (\kappa \gamma_P \delta_P - \delta_P \gamma'_P + \gamma'_P))}{\varepsilon m_P (m_P + \gamma_P) (m_P + \omega_P) (m_P + \gamma'_P)} \\ &\quad + \frac{\omega_P \beta_W (m_P (\delta_P \mu'_P - \delta_P \mu_P + \mu_P) + (\delta_P - 1) \mu_P (-\gamma'_P) + \gamma_P \delta_P \mu'_P)}{\varepsilon m_P (m_P + \gamma_P) (m_P + \omega_P) (m_P + \gamma'_P)} = 0.003913 > 0 \\ \frac{\partial \mathbb{R}_0}{\partial \varepsilon} &= \frac{\Lambda_P \omega_P \beta_W (m_P ((\delta_P - 1) \mu_P - \delta_P \mu'_P) + (\delta_P - 1) \mu_P \gamma'_P - \gamma_P \delta_P \mu'_P)}{\varepsilon^2 m_P (m_P + \gamma_P) (m_P + \omega_P) (m_P + \gamma'_P)} = -0.0163414 < 0 \\ \frac{\partial \mathbb{R}_0}{\partial \beta_P} &= \frac{\Lambda_P \omega_P (m_P ((\kappa - 1)\delta_P + 1) + \kappa \gamma_P \delta_P + (\delta_P - 1) (-\gamma'_P))}{m_P (m_P + \gamma_P) (m_P + \omega_P) (m_P + \gamma'_P)} = 37935.3 > 0 \end{aligned}$$

$$\begin{aligned}
\frac{\partial \mathbb{R}_0}{\partial \gamma'_P} &= -\frac{\delta_P \Lambda_P \omega_P (\varepsilon \kappa \beta_P + \beta_W \mu'_P)}{\varepsilon m_P (m_P + \omega_P) (m_P + \gamma'_P)^2} = -0.0784132 < 0 \\
\frac{\partial \mathbb{R}_0}{\partial \kappa} &= \frac{\beta_P \delta_P \Lambda_P \omega_P}{m_P (m_P + \omega_P) (m_P + \gamma'_P)} = 0.029181 > 0 \\
\frac{\partial \mathbb{R}_0}{\partial \gamma_P} &= \frac{(\delta_P - 1) \Lambda_P \omega_P (\varepsilon \beta_P + \mu_P \beta_W)}{\varepsilon m_P (m_P + \gamma_P)^2 (m_P + \omega_P)} = -2.91855 < 0 \\
\frac{\partial \mathbb{R}_0}{\partial \delta_P} &= \frac{\Lambda_P \omega_P (m_P (\varepsilon (\kappa - 1) \beta_P + \beta_W (\mu'_P - \mu_P)) + \varepsilon \beta_P (\kappa \gamma_P - \gamma'_P) + \beta_W (\gamma_P \mu'_P - \mu_P \gamma'_P))}{\varepsilon m_P (m_P + \gamma_P) (m_P + \omega_P) (m_P + \gamma'_P)} \\
&= -0.286363 < 0 \\
\frac{\partial \mathbb{R}_0}{\partial \beta_W} &= \frac{\Lambda_P \omega_P (m_P (\delta_P \mu'_P - (\delta_P - 1) \mu_P) + \gamma_P \delta_P \mu'_P + (\delta_P - 1) \mu_P (-\gamma_P))}{\varepsilon m_P (m_P + \gamma_P) (m_P + \omega_P) (m_P + \gamma'_P)} = 46.6896 > 0 \\
\frac{\partial \mathbb{R}_0}{\partial \mu_P} &= \frac{(1 - \delta_P) \Lambda_P \omega_P \beta_W}{\varepsilon m_P (m_P + \gamma_P) (m_P + \omega_P)} = 12.9369 > 0 \\
\frac{\partial \mathbb{R}_0}{\partial \mu'_P} &= \frac{\delta_P \Lambda_P \omega_P \beta_W}{\varepsilon m_P (m_P + \omega_P) (m_P + \gamma'_P)} = 0.68089 > 0 \\
\frac{\partial \mathbb{R}_0}{\partial \omega_P} &= \frac{\beta_P \Lambda_P (\varepsilon m_P ((\kappa - 1) \delta_P + 1) + \varepsilon (\kappa \gamma_P \delta_P - (\delta_P - 1) \gamma'_P))}{\varepsilon (m_P + \gamma_P) (m_P + \omega_P)^2 (m_P + \gamma'_P)} \\
&\quad + \frac{\Lambda_P \beta_W (m_P (\delta_P \mu'_P + (1 - \delta_P) \mu_P) + (\delta_P - 1) \mu_P (-\gamma'_P) + \gamma_P \delta_P \mu'_P)}{\varepsilon (m_P + \gamma_P) (m_P + \omega_P)^2 (m_P + \gamma'_P)} = 0.254 > 0
\end{aligned}$$

It's clear that, the reproductive number \mathbb{R}_0 increases with the increment of parameters $\Lambda_P, \beta_P, \kappa, \beta_W, \mu_P, \mu'_P, \omega_P$ and decreases with parameters $\varepsilon, \gamma_P, \gamma'_P$.

3 SKAZI scheme

In order to compute the analytic solution of differential equations, we face some difficulties. One of major difficulty is that, the non-linearity behavior of differential equation. Additionally, there is no such exact formula while computation of the exact solution. To tackle and solve such type of non-linearity, we use some numerical integration schemes to get the approximate solution.

Suppose we are dealing by initial value problem as given in model (1) and would like to resolve the model in a closed interval $[t_0, t_N]$. For this intention, we partitioned the interval $[t_0, t_N]$ with equi-spaced step size h . This can be made by means of mesh points i.e. $t_k = t_0 + kh$ for all $k = 0 : N$ such that $h = (t_N - t_0)/N$ for positive integer N . In this intellect, we suppose that for each n we obtain a numerical approximation $Y^{(k)}$ in relevant with $Y(t_k)$, that is the analytic solution at a point t_k . For a certain initial value problem with $Y(t_0) = Y^{(0)}$, we define,

$$Y^{(k+1)} = Y^{(k)} + h\Psi(Y^{(k)}; h), \quad k = 0 : N \quad (14)$$

where the term $\Psi(Y^{(k)}; h)$ is uncertainty level and given as follows,

$$\Psi(Y^{(k)}; h) = \zeta \left(\Psi_1(Y^{(k)}) + \Psi_3(\Psi_2; h) \right) \quad (15)$$

where $\zeta \in (0, 1)$, $\Psi_1(Y^{(k)}) = Y'$, $\Psi_3(\Psi_2; h) = \Psi_1(\Psi_2; h)$ and $\Psi_2(Y^{(k)}; h) = Y^{(k)} + h\Psi_1(Y^{(k)})$. The uncertainty level $\Psi(Y^{(k)}; h)$ is a continuous function as $\Psi_1(Y^{(k)})$, $\Psi_2(Y^{(k)}; h)$ and $\Psi_3(Y^{(k)}; h)$ are continuous. For the purpose of accuracy and convergence of SKAZI scheme, we introduced two results based on the global error and truncation error. The global error \mathbb{GE}_k of SKAZI scheme is defined as follows,

$$\mathbb{GE}_k = Y^{(k+1)} - Y_k, \quad (16)$$

where $Y^{(k)}$ and Y_k represent the approximate and analytic solution respectively. The truncation error \mathbb{TE}_k for SKAZI scheme along with uncertainty level $\Psi(Y^{(k)}; h)$ is defined as follows,

$$\mathbb{TE}_k = \left| \Psi(Y^{(k)}; h) - \frac{Y^{(k+1)} - Y^{(k)}}{h} \right| \quad (17)$$

where $|\cdot|$ is the absolute modulus. The bounds of global error along with mixture of truncation error is formulated by following Theorem 3.1.

Theorem 3.1 Suppose a general method (14) along with continuity of uncertainty level $\Psi(Y; h) = \Psi(t, Y; h)$ around its arguments. Further assume that $\Psi(Y; h)$ holds for Lipschitz condition in its neighbour of secondary argument. For region Ω which enclose a parallelepiped;

$$\Omega = \{(t, Y) : t_0 \leq t \leq t_N, \|Y - Y_0\| \leq Y_N\} \quad (18)$$

with constant $t_N > t_0$, $Y_N > 0$ and $h \in [0, h_0]$, there exist Lipschitz constant L_Ψ such that,

$$|\Psi(t, Y; h) - \Psi(t, Z; h)| \leq L_\Psi |Y - Z| \quad \text{for } (t, Y), (t, Z) \in \Omega \quad (19)$$

Then the bounds $|Y_k - Y_0| \leq Y_N$, yields that

$$|\mathbb{GE}| \leq e^{L_\Psi(t_k - t_0)} |\mathbb{GE}_0| + \mathbb{TE} \left[\frac{e^{L_\Psi(t_k - t_0)} - 1}{L_\Psi} \right] \quad (20)$$

where $\mathbb{TE} = \max_{0 \leq k \leq N-1} |\mathbb{TE}_k|$ for all $k = 0 : N$.

Assumption

Suppose that the Theorem 3.1 holds and if truncation error \mathbb{TE}_k tends to zero as step-size h tends to zero then global error \mathbb{GE} tends to zero.

The general numerical scheme (14) is said to be consistent with $Y' = \Psi_1(Y^{(k)})$ along with truncation error \mathbb{TE}_k if for any $\zeta > 0$ there exist a step-size valued function $h(\zeta)$ which is of course positive and region Ω encloses all pair points $(t_k, Y^{(k)})$, $(t_{k+1}, Y^{(k+1)})$ on its

graphical simulation. Since the uncertainty level is continuous in $[t_0, t_k]$, this provides $Y'(t_k)$ continuous. Thus for a very small step-size h , the truncation error \mathbb{TE}_k (17) becomes,

$$\mathbb{TE}_k = Y'(t_k) - \Psi(t_k, Y^{(k)}; 0). \quad (21)$$

The \mathbb{TE}_k (21) along with numerical scheme (14) is consistent iff

$$\Psi(t_k, Y^{(k)}; 0) = \Psi_1(y). \quad (22)$$

Theorem 3.2 *Let assumption (3) be hold and approximate solution (14) of initial value problem $Y'(t) = \Psi_1(t, Y(t_0))$ with $Y(t_0) = Y^{(0)}$ enclosed by the region Ω such that the step-size $h \leq h_0$. Further assume that the uncertainty level $\Psi(".; ".)$ is uniformly continuous on $\Omega \times [0, h_0]$ and it holds for (22) and Lipschitz condition,*

$$|\Psi(t, Y; h) - \Psi(t, Z; h)| \leq L_\Psi |Y - Z| \quad (23)$$

Then series of approximate solution $Y^{(k)}$ along with respective series of $t_k = t_0 + kh$ for $k = 0 : N$ such that step-size h successively decreases to h_0 , converges to analytic solution of initial value problem, that is

$$|Y^{(k)} - Y_k| \rightarrow 0 \quad h \rightarrow 0, t_k \rightarrow t \in [t_0, t_k]. \quad (24)$$

3.1 Proposed SKAZI scheme

Next, we apply the SKAZI scheme on the non-linear model (1) in order to approximate the solution. The non-linear terms is modeled by introducing sub-functions in $\Psi(".; h)$ like we modeled $S_P W = S_P^{(k+1)} W^k$ instead of $S_P W = S_P^{(k)} W^{(k)}$ in $\Psi_1(".)$, first equation of system (25). To construct the discrete formulation of SKAZI scheme of non-linear model (1), we formulate $\Psi_1(".)$ and $\Psi_2(".; h)$. The uncertainty level $\Psi(".; h)$ for mathematical model (1) is formulated as follows,

$$\begin{aligned} \Psi_1(S_P^{(k+1)}) &= \Lambda_P - \beta_P S_P^{(k+1)} \left(\kappa A_P^{(k)} + I_P^{(k)} \right) - m_P S_P^{(k+1)} - \beta_W W^{(k)} S_P^{(k+1)} \\ \Psi_1(E_P^{(k+1)}) &= \beta_P S_P^{(k+1)} \left(\kappa A_P^{(k)} + I_P^{(k)} \right) - E_P^{(k+1)} (m_P + (1 - \delta_P) \omega_P + \delta_P \omega'_P) + \beta_W W^{(k)} S_P^{(k+1)} \\ \Psi_1(I_P^{(k+1)}) &= E_P^{(k+1)} (1 - \delta_P) \omega_P - I_P^{(k+1)} (m_P + \gamma_P) \\ \Psi_1(A_P^{(k+1)}) &= E_P^{(k+1)} \delta_P \omega'_P - A_P^{(k+1)} (m_P + \gamma'_P) \\ \Psi_1(R_P^{(k+1)}) &= A_P^{(k+1)} \gamma'_P + I_P^{(k+1)} \gamma_P - m_P R_P^{(k+1)} \\ \Psi_1(W^{(k+1)}) &= A_P^{(k+1)} \mu'_P + I_P^{(k+1)} \mu_P - \varepsilon W^{(k+1)} \end{aligned} \quad (25)$$

The function $\Psi_2(".;h)$ can be formulated using (15) along with $\Psi_1(".;h)$ as follows,

$$\begin{aligned}
\Psi_2(S_P^{(k+1)};h) &= S_P^{(k+1)} + h \left(\Lambda_P - \beta_P S_P^{(k+1)} \left(\kappa A_P^{(k)} + I_P^{(k)} \right) - m_P S_P^{(k+1)} - \beta_W W^{(k)} S_P^{(k+1)} \right) \\
\Psi_2(E_P^{(k+1)};h) &= E_P^{(k+1)} + h \beta_P S_P^{(k+1)} \left(\kappa A_P^{(k)} + I_P^{(k)} \right) - h E_P^{(k+1)} (m_P + (1 - \delta_P) \omega_P + \delta_P \omega'_P) \\
&\quad + h \beta_W W^{(k)} S_P^{(k+1)} \\
\Psi_2(I_P^{(k+1)};h) &= I_P^{(k+1)} + h \left(E_P^{(k+1)} (1 - \delta_P) \omega_P - I_P^{(k+1)} (m_P + \gamma_P) \right) \\
\Psi_2(A_P^{(k+1)};h) &= A_P^{(k+1)} + h \left(E_P^{(k+1)} \delta_P \omega'_P - A_P^{(k+1)} (m_P + \gamma'_P) \right) \\
\Psi_2(R_P^{(k+1)};h) &= R_P^{(k+1)} + h \left(A_P^{(k+1)} \gamma'_P + I_P^{(k+1)} \gamma_P - m_P R_P^{(k+1)} \right) \\
\Psi_2(W^{(k+1)};h) &= W^{(k+1)} + h \left(A_P^{(k+1)} \mu'_P + I_P^{(k+1)} \mu_P - \varepsilon W^{(k+1)} \right)
\end{aligned}$$

The function $\Psi_3(".;h)$ in term of $\Psi_1(\Psi_2(".;h))$ can be evaluated as follows,

$$\begin{aligned}
\Psi_3(S_P^{(k+1)};h) &= \Psi_1(\Psi_2(S_P^{(k+1)};h)) \\
&= \Lambda_P - \beta_P \Psi_2(S_P^{(k+1)};h) \left(\kappa A_P^{(k)} + I_P^{(k)} \right) - m_P \Psi_2(S_P^{(k+1)};h) - \beta_W W^{(k)} \Psi_2(S_P^{(k+1)};h) \\
&= \left(h \left(\beta_P \left(\kappa A_P^{(k)} + I_P^{(k)} \right) + W^{(k)} \beta_W + m_P \right) - 1 \right) \\
&\quad \times \left(S_P^{(k+1)} \left(\beta_P \left(\kappa A_P^{(k)} + I_P^{(k)} \right) + W^{(k)} \beta_W + m_P \right) - \Lambda_P \right) \\
\Psi_3(E_P^{(k+1)};h) &= \Psi_1(\Psi_2(E_P^{(k+1)};h)) \\
&= \beta_P S_P^{(k+1)} \left(\kappa A_P^{(k)} + I_P^{(k)} \right) - \Psi_2(E_P^{(k+1)};h) (m_P + (1 - \delta_P) \omega_P + \delta_P \omega'_P) + \beta_W W^{(k)} S_P^{(k+1)} \\
&= h \left((m_P + \omega_P (1 - \delta_P) + \delta_P \omega'_P) - 1 \right) \times \\
&\quad \left(E_P^{(k+1)} (m_P - \delta_P \omega_P + \delta_P \omega'_P + \omega_P) - S_P^{(k+1)} \left(\kappa \beta_P A_P^{(k)} + \beta_P I_P^{(k)} + W^{(k)} \beta_W \right) \right) \\
\Psi_3(I_P^{(k+1)};h) &= \Psi_1(\Psi_2(I_P^{(k+1)};h)) \\
&= E_P^{(k+1)} (1 - \delta_P) \omega_P - \Psi_2(I_P^{(k+1)};h) (m_P + \gamma_P) \\
&= (h (m_P + \gamma_P) - 1) \left((\delta_P - 1) \omega_P E_P^{(k+1)} + I_P^{(k+1)} (m_P + \gamma_P) \right) \\
\Psi_3(A_P^{(k+1)};h) &= \Psi_1(\Psi_2(A_P^{(k+1)};h)) \\
&= E_P^{(k+1)} \delta_P \omega'_P - \Psi_2(A_P^{(k+1)};h) (m_P + \gamma'_P) \\
&= (h (m_P + \gamma'_P) - 2) \left(A_P^{(k+1)} (m_P + \gamma'_P) - \delta_P \omega'_P E_P^{(k+1)} \right) \\
\Psi_3(R_P^{(k+1)};h) &= \Psi_1(\Psi_2(R_P^{(k+1)};h)) \\
&= A_P^{(k+1)} \gamma'_P + I_P^{(k+1)} \gamma_P - m_P \Psi_2(R_P^{(k+1)};h) \\
&= (h (m_P + \gamma'_P) - 1) \left(A_P^{(k+1)} (m_P + \gamma'_P) - \delta_P \omega'_P E_P^{(k+1)} \right)
\end{aligned}$$

$$\begin{aligned}
\Psi_3(W^{(k+1)}; h) &= \Psi_1(\Psi_2(W^{(k+1)}; h)) \\
&= A_P^{(k+1)} \mu'_P + I_P^{(k+1)} \mu_P - \varepsilon \Psi_2(W^{(k+1)}) \\
&= (hm_P - 1) \left(-\gamma'_P A_P^{(k+1)} - \gamma_P I_P^{(k+1)} + m_P R_P^{(k+1)} \right)
\end{aligned}$$

The discrete system of ordinary differential equation (1) along with uncertainty level $\Psi(\cdot; h)$ given as follows,

$$\begin{aligned}
\frac{S_P^{(k+1)} - S_P^{(k)}}{h} &= \zeta(\Psi(S_P^{(k+1)}; h)) = \zeta(\Psi_1(S_P^{(k+1)}) + \Psi_3(S_P^{(k+1)}; h)) \\
\frac{E_P^{(k+1)} - E_P^{(k)}}{h} &= \zeta(\Psi(E_P^{(k+1)}; h)) = \zeta(\Psi_1(E_P^{(k+1)}) + \Psi_3(E_P^{(k+1)}; h)) \\
\frac{I_P^{(k+1)} - I_P^{(k)}}{h} &= \zeta(\Psi(I_P^{(k+1)}; h)) = \zeta(\Psi_1(I_P^{(k+1)}) + \Psi_3(I_P^{(k+1)}; h)) \\
\frac{A_P^{(k+1)} - A_P^{(k)}}{h} &= \zeta(\Psi(A_P^{(k+1)}; h)) = \zeta(\Psi_1(A_P^{(k+1)}) + \Psi_3(A_P^{(k+1)}; h)) \\
\frac{R_P^{(k+1)} - R_P^{(k)}}{h} &= \zeta(\Psi(R_P^{(k+1)}; h)) = \zeta(\Psi_1(R_P^{(k+1)}) + \Psi_3(R_P^{(k+1)}; h)) \\
\frac{W^{(k+1)} - W^{(k)}}{h} &= \zeta(\Psi(W^{(k+1)}; h)) = \zeta(\Psi_1(W^{(k+1)}) + \Psi_3(W^{(k+1)}; h))
\end{aligned} \tag{26}$$

For $\zeta = 1/2$, the above equation (26) can be simplified as follows,

$$\begin{aligned}
S_P^{(k+1)} &= \frac{-2S_P^{(k)} + h\Lambda_P(-2 + h(\beta_P(I_P^{(k)} + A_P^{(k)}\kappa) + m_P + \beta_W W^{(k)}))}{-2 + h(\beta_P(I_P^{(k)} + A_P^{(k)}\kappa) + m_P + \beta_W W^{(k)})(-2 + h(\beta_P(I_P^{(k)} + A_P^{(k)}\kappa) + m_P + \beta_W W^{(k)}))} \\
E_P^{(k+1)} &= \frac{-2E_P^{(k)} + h(-2 + h(m_P + \omega_P - \delta_P \omega_P + \delta_P \omega'_P))S_P^{(k+1)}(\beta_P(I_P^{(k)} + A_P^{(k)}\kappa) + \beta_W W^{(k)})}{-2 + h(m_P - (-1 + \delta_P)\omega_P + \delta_P \omega'_P)(-2 + h(m_P - (-1 + \delta_P)\omega_P + \delta_P \omega'_P))} \\
I_P^{(k+1)} &= \frac{-(2I_P^{(k)} + (-1 + \delta_P)E_P^{(k+1)})h(-2 + h(\gamma_P + m_P))\omega_P}{-2 + h(\gamma_P + m_P)(-2 + h(\gamma_P + m_P))} \\
A_P^{(k+1)} &= \frac{2A_P^{(k)} + 2\delta_P E_P^{(k+1)}h\omega_P - \delta_P E_P^{(k+1)}\gamma'_P h^2 \omega_P - \delta_P E_P^{(k+1)}h^2 m_P \omega_P}{2 + 2\gamma'_P h - \gamma_P'^2 h^2 + 2hm_P - 2\gamma'_P h^2 m_P - h^2 m_P^2} \\
R_P^{(k+1)} &= \frac{-2A_P^{(k+1)}\gamma'_P h - 2\gamma_P h I_P^{(k+1)} + A_P^{(k+1)}\gamma'_P h^2 m_P + \gamma_P h^2 I_P^{(k+1)} m_P - 2R_P^{(k)}}{-2 - 2hm_P + h^2 m_P^2} \\
W^{(k+1)} &= \frac{-2hI_P^{(k)}\mu_P + \varepsilon h^2 I_P^{(k+1)}\mu_P - 2A_P^{(k+1)}h\mu'_P + AP(n+1)\varepsilon h^2 \mu'_P - 2W^{(k)}(n)}{-2 - 2\varepsilon h + \varepsilon^2 h^2}
\end{aligned} \tag{27}$$

Table 2: The parameters of SAR-CoV-2 infection model (1) for disease free equilibrium point. Note that the value of N_P is taken from WHO [https://www.who.int/redirect-pages/page/novel-coronavirus-\(covid-19\)-situation-dashboard](https://www.who.int/redirect-pages/page/novel-coronavirus-(covid-19)-situation-dashboard)

| Symbol | Description | values | |
|---------------|--|----------------------|---------|
| ω_P | The rate of incubation period of people | 1/5.2 | [2] |
| ω'_P | The rate of latent period of people | 1/5.2 | [2] |
| γ_P | The rate of infectious period of symptomatic infection of people | 1/5.8 | [2] |
| γ'_P | The rate of infectious period of symptomatic infection of people | 1/5.8 | [2] |
| δ_P | The proportion of asymptomatic infection rate of people | 0.5 | [2] |
| β_P | The transmission rate from I_P to S_P | 0.000015 | Assumed |
| β_W | The transmission rate from W to S_P | 0.000035 | Assumed |
| μ_P | The shedding coefficients from I_P to W | 0.0001 | Assumed |
| μ'_P | The shedding coefficients from A_P to W | 0.00005 | Assumed |
| κ | The multiple of the transmissibility of A_P to that of I_P | 0.5 | [2] |
| m_P | The death rate of people | 0.2/11 | [2] |
| ε | The rate lifetime of the virus in W | 1/10 | [2] |
| N_P | Total number of people (confirmed cases) | 81761 | WHO |
| Λ_P | Rate of recruiting the susceptible SAR-CoV-2 per unit time. | $\frac{N_P m_P}{10}$ | [2] |

Table 3: The parameters of SAR-CoV-2 infection model (1) for endemic equilibrium point. Note that the value of N_P is taken from WHO [https://www.who.int/redirect-pages/page/novel-coronavirus-\(covid-19\)-situation-dashboard](https://www.who.int/redirect-pages/page/novel-coronavirus-(covid-19)-situation-dashboard)

| Symbol | Description | values | |
|---------------|--|----------------------|---------|
| ω_P | The rate of incubation period of people | 1/5.2 | [2] |
| ω'_P | The rate of latent period of people | 1/5.2 | [2] |
| γ_P | The rate of infectious period of symptomatic infection of people | 1/5.8 | [2] |
| γ'_P | The rate of infectious period of symptomatic infection of people | 1/5.8 | [2] |
| δ_P | The proportion of asymptomatic infection rate of people | 0.5 | [2] |
| β_P | The transmission rate from I_P to S_P | 0.000095 | Assumed |
| β_W | The transmission rate from W to S_P | 0.000035 | Assumed |
| μ_P | The shedding coefficients from I_P to W | 0.0001 | Assumed |
| μ'_P | The shedding coefficients from A_P to W | 0.00005 | Assumed |
| κ | The multiple of the transmissibility of A_P to that of I_P | 0.5 | [2] |
| m_P | The death rate of people | 0.2/11 | [2] |
| ε | The rate lifetime of the virus in W | 1/10 | [2] |
| N_P | Total number of people (confirmed cases) | 81761 | WHO |
| Λ_P | Rate of recruiting the susceptible SAR-CoV-2 per unit time. | $\frac{N_P m_P}{10}$ | [2] |

4 Numerical implementation

In this section, we present the approximate solution of considered model (1) using our new SKAZI scheme. All the numerical tests are executed using MATLAB (R2016a) on the laptop Intel(R) Core(TM) i5 CPU M20 @ 2.40GHz 2.40 GHz 2.00 GB RAM. The MATLAB codes of Scheme is available at <https://sites.google.com/site/sadaqateshu>.

The Figure.2 give numerical results of susceptible population $S_P(t)$ computed by SKAZI scheme for disease free equilibrium points such that $\mathbb{R}_0 < 1$. The numeric approximations of $S_P(t)$ tend to $\frac{\Lambda_P}{\mu_T}$, that is rate of recruiting the susceptible SAR-CoV-2 per unit time and rate of decaying (rate of people traveling out) in susceptible $S_P(t)$ per unit time. To analyzed more effects for $S_P(t)$ at $\mathbb{R}_0 < 1$, we variate the parameters m_P and apply SKAZI scheme. We note that the risk of SAR-CoV-2 to other people increases with increment of rate of people traveling out from the susceptible population $S_P(t)$. But, by this effects remains the susceptible population $S_P(t)$ in infection free situation for all situations (lock down or heavy rush of population).

The Figure.3 give numerical results of exposed population $E_P(t)$ computed by SKAZI scheme for disease free equilibrium points such that $\mathbb{R}_0 < 1$. The exposed population is directly connected with the transmission rate of infection of SAR-CoV-2 reservoir $W(t)$ to susceptible population $S_P(t)$, that is, β_W . By increasing β_W , the exposed population $E_P(t)$ tends toward the endemic equilibrium point and at point $\beta \leq 0.0182957$ the exposed population $E_P(t)$ still remains infection free.

The Figure.4-5 give numerical results of symptomatic and asymptomatic infected population $I_P(t)$ and $A_P(t)$ respectively, computed by SKAZI scheme for disease free equilibrium points such that $\mathbb{R}_0 < 1$. The infection of SAR-CoV-2 with infected compartment $I_P(t)$ becomes very effective with rate of delay from symptom onset to detection/hospitalization, that is, γ and γ' . The results shows that the infected population tends towards endemic with increments of γ and γ' . This means that, if the delay is added in infected population to detection or hospitalization process the infection becomes more maniac. For intense, for delay less than 15 days the disease becomes remain infection free. But, if the infected people gets delay more than 15 days the case becomes sensitive and treated as endemic or incurable.

The Figure.6 give numerical results of removed population (recovered and death) $R_P(t)$ computed by SKAZI scheme for disease free equilibrium points such that $\mathbb{R}_0 < 1$. The recovery of infected population is variate with the variation of rate of moving in or traveling out of the population region. The result shows that at stage of parameter (Table.??), the $R_P(t)$ decreases more fast with increment of traveling out of region, that is, m_P .

The Figure.7 give numerical results of SARS-CoV-2 in reservoir population $W(t)$ computed by SKAZI scheme for disease free equilibrium points such that $\mathbb{R}_0 < 1$. In seafood market, the compartment $W(t)$ is directly related with life time of SARS-CoV-2. The SARS-CoV-2 stay for a longer time (10 days) in the unknown hosts in market that is ε . We variate the stay time of SAR-CoV-2 in an unknown host. The compartment $W(t)$ converges

rapidly towards infection free status, when we take action quickly against transmission of SARS-CoV-2. The $W(t)$ tends toward endemic infection for all values greater than $\varepsilon \geq 553$.

Now a days, the SARS-CoV-2 is rapidly increases and becomes endemic in society. Therefore, we are interesting to analyze the epidemic behavior of SARS-CoV-2 under the consideration of different parameters given in Table.3. We formulate analytic solution (2) and numeric solution obtained by SKAZI scheme (2) of model (1).

In Figure.7, we investigate that the risk of SAR-CoV-2 to other people increases with increment of rate of people traveling out from the susceptible population $S_P(t)$. If the traveling out rate m_P posses a directly relation to susceptible population $S_P(t)$. If the rate of people traveling out is increasing the susceptible $S_P(t)$ tends to infection free state. This means that if we set lock down in an entire region the susceptible population $S_P(t)$ is still remain endemic. The susceptible population $S_P(t)$ tends toward infection free for people 1.662 million traveling out to the total population according to considered model.

The population $E_P(t)$ exposed by SARS-CoV-2 increases with increment of transmission rate from W to S_P depicted in Figure 9. The exposed population remains endemic over all values of β_W and infection becomes more sensitive with large increment of β_W .

The infection of SAR-CoV-2 with infected compartment $I_P(t)$ and $A_P(t)$ rapidly increasing by delaying from symptom onset to detection/hospitalization, that is, γ and γ' respectively, illustrated in Figure.10-11. By considered model, the infected population tends towards higher endemic case with increments of γ and γ' . This means that, if the delay is added in infected population to detection or hospitalization process the infection becomes more maniac. For instance, the delay less than 2 day the disease becomes infection free. But, if the infected people gets delay more than 1 day the case becomes sensitive and treated as endemic or incurable.

The recovered and total death $R_P(t)$ decreases with increment of traveling out or death rate respectively as given in Figure.12. The Figure.13 give numerical results of SARS-CoV-2 in reservoir population $W(t)$. In seafood market, the compartment $W(t)$ is directly related with life time of SARS-CoV-2. The SARS-CoV-2 stay for a longer time (10 days) in the unknown hosts in market that is ε . We variate the stay time of SAR-CoV-2 in an unknown host and results shows a slightly change in endemic behavior of seafood market.

Figure 2: Numerical results of susceptible population $S_P(t)$ with variation of m_P computed by SKAZI scheme along with step size $h = 0.001$ for disease free equilibrium points such that $\mathbb{R}_0 < 1$.

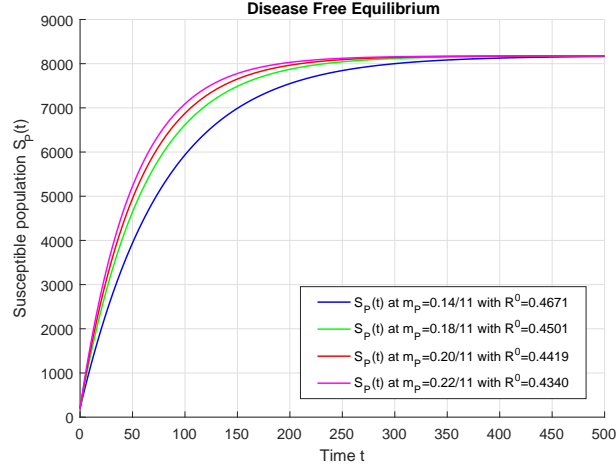


Figure 3: Numerical results of exposed population $E_P(t)$ with variation of β_W computed by SKAZI scheme along with step size $h = 0.001$ for disease free equilibrium points such that $\mathbb{R}_0 < 1$.

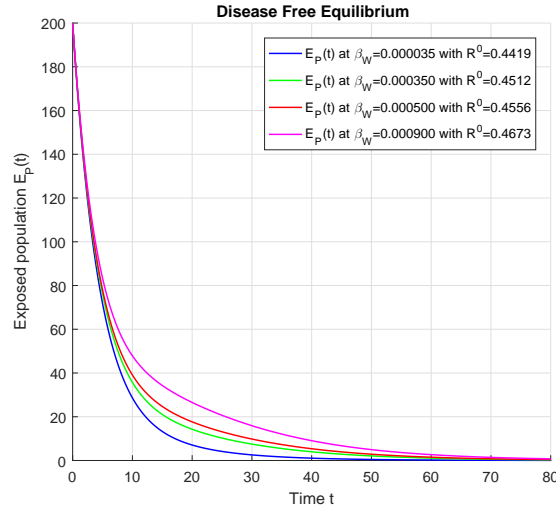


Figure 4: Numerical results of symptomatic infected population $I_P(t)$ with variation of γ_P and γ'_P computed by SKAZI scheme along with step size $h = 0.001$ for disease free equilibrium points such that $\mathbb{R}_0 < 1$.

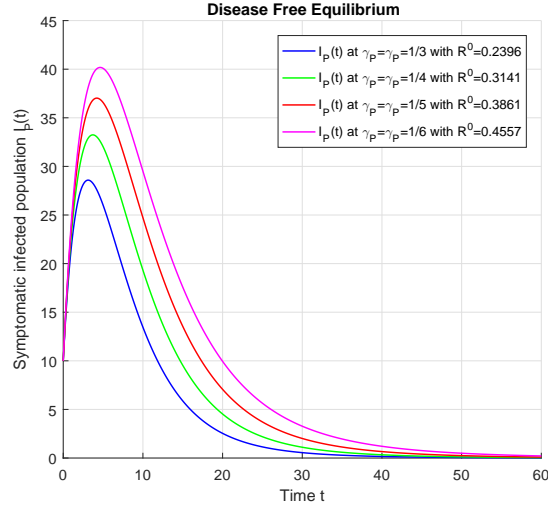


Figure 5: Numerical results of asymptomatic infected population $A_P(t)$ with variation of γ_P and γ'_P computed by SKAZI scheme along with step size $h = 0.001$ for disease free equilibrium points such that $\mathbb{R}_0 < 1$.

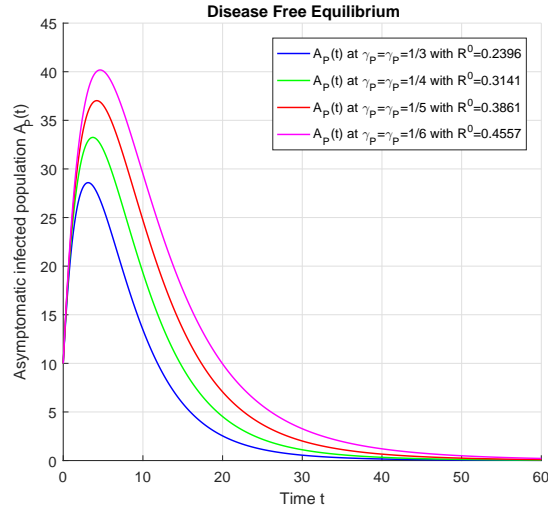


Figure 6: Numerical results of removed (recovered and death) population $R_P(t)$ with variation of m_P computed by SKAZI scheme along with step size $h = 0.001$ for disease free equilibrium points such that $\mathbb{R}_0 < 1$.

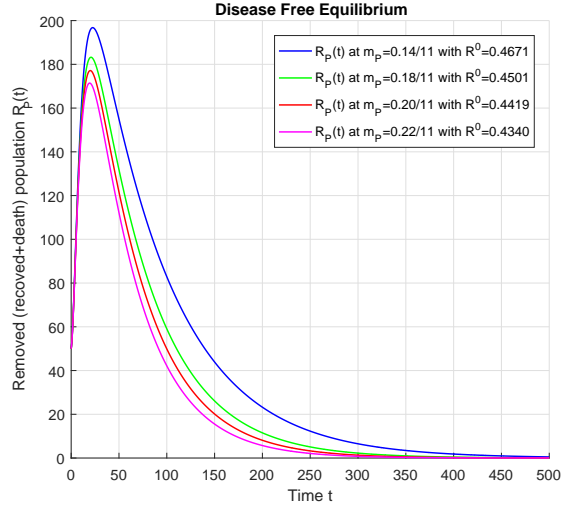


Figure 7: Numerical results of SARS-CoV-2 in reservoir (the seafood market) population $W(t)$ with variation of ε computed by SKAZI scheme along with step size $h = 0.001$ for disease free equilibrium points such that $\mathbb{R}_0 < 1$.

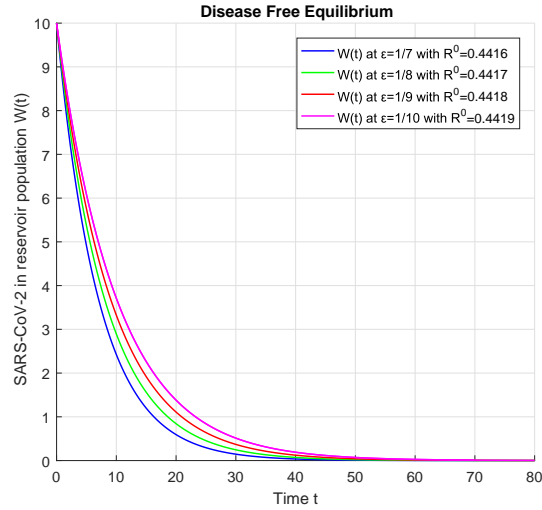


Figure 8: Numerical results of susceptible population $S_P(t)$ with variation of m_P computed by SKAZI scheme along with step size $h = 0.001$ for endemic equilibrium points such that $\mathbb{R}_0 < 1$.

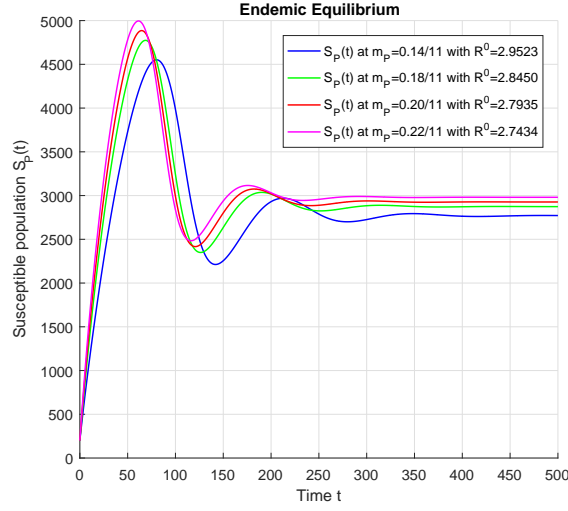


Figure 9: Numerical results of exposed population $E_P(t)$ with variation of β_W computed by SKAZI scheme along with step size $h = 0.001$ for endemic equilibrium points such that $\mathbb{R}_0 > 1$.

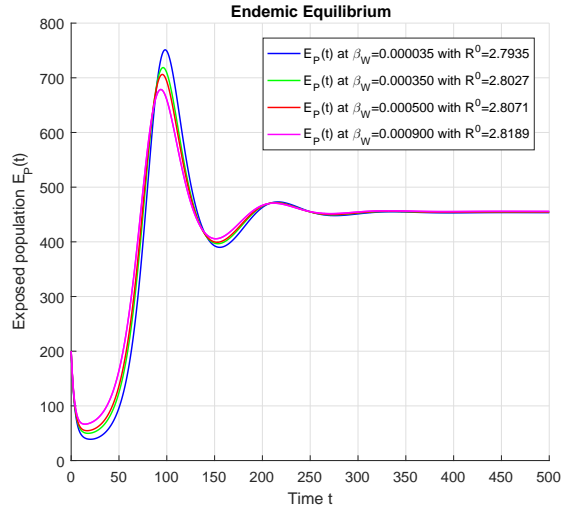


Figure 10: Numerical results of symptomatic infected population $I_P(t)$ with variation of γ_P and γ'_P computed by SKAZI scheme along with step size $h = 0.001$ for endemic equilibrium points such that $\mathbb{R}_0 > 1$.

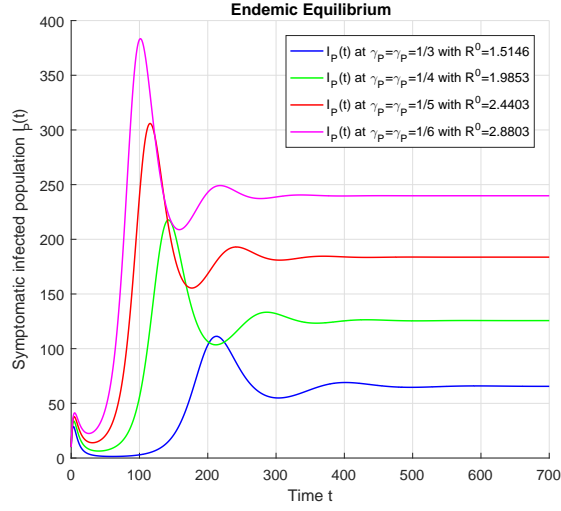


Figure 11: Numerical results of asymptomatic infected population $A_P(t)$ with variation of γ_P and γ'_P computed by SKAZI scheme along with step size $h = 0.001$ for endemic equilibrium points such that $\mathbb{R}_0 > 1$.

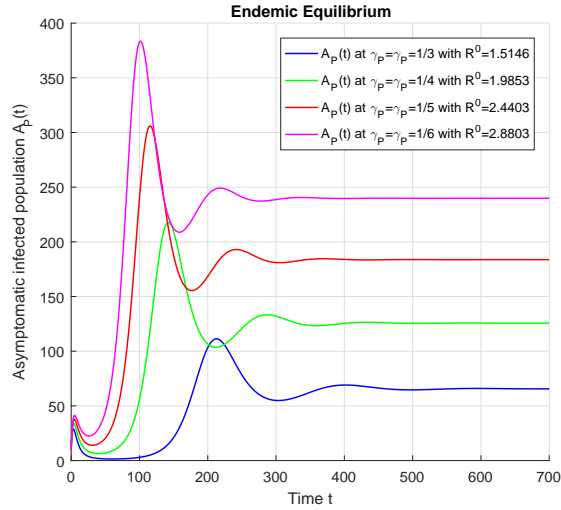


Figure 12: Numerical results of removed (recovered and death) population $R_P(t)$ with variation of m_P computed by SKAZI scheme along with step size $h = 0.001$ for endemic equilibrium points such that $\mathbb{R}_0 > 1$.

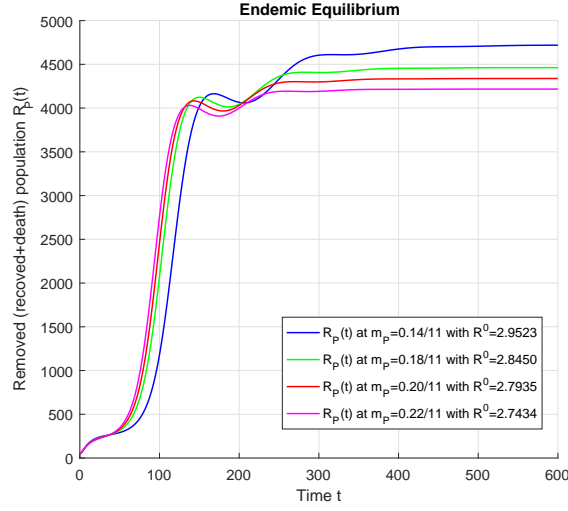
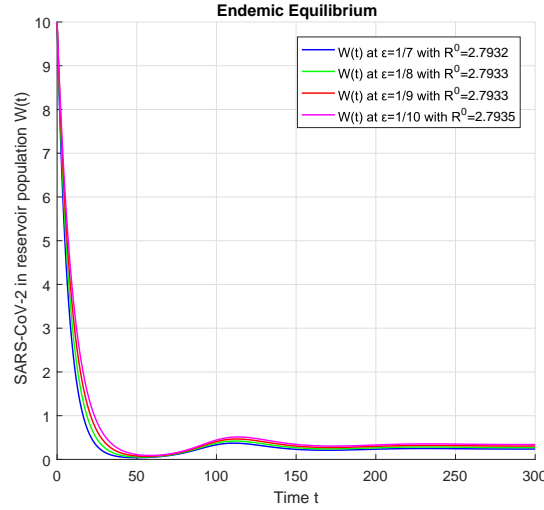


Figure 13: Numerical results of SARS-CoV-2 in reservoir (the seafood market) population $W(t)$ with variation of ε computed by SKAZI scheme along with step size $h = 0.001$ for endemic equilibrium points such that $\mathbb{R}_0 > 1$.



Conclusion

In this article, a mathematical model of SARS-CoV-2 for transmissibility is presented. The disease free and endemic equilibrium points are evaluated. The stability analysis of SARS-CoV-2 model is established. The basic reproduction number \mathbb{R}^0 is formulated using next generation approach. Also, we proposed an efficient SKAZI scheme to approximate the solution (both disease free and endemic equilibrium) of considered model (1).

Acknowledgment

We would like to thank the reviewers for their comments and insightful feedback that helped us to improve the paper significantly.

References

- [1] Carlos, W. G., Dela Cruz, C. S., Cao, B., Pasnick, S., and Jamil, S. (2020). Novel wuhan (2019-ncov) coronavirus. *American journal of respiratory and critical care medicine*, 201(4):P7–P8.
- [2] Chen, T.-M., Rui, J., Wang, Q.-P., Zhao, Z.-Y., Cui, J.-A., and Yin, L. (2020). A mathematical model for simulating the phase-based transmissibility of a novel coronavirus. *Infectious Diseases of Poverty*, 9(1):1–8.
- [3] Killerby, M. E., Biggs, H. M., Midgley, C. M., Gerber, S. I., and Watson, J. T. (2020). Middle east respiratory syndrome coronavirus transmission. *Emerging infectious diseases*, 26(2):191.
- [4] Li, Q., Guan, X., Wu, P., Wang, X., Zhou, L., Tong, Y., Ren, R., Leung, K. S., Lau, E. H., Wong, J. Y., et al. (2020). Early transmission dynamics in wuhan, china, of novel coronavirus–infected pneumonia. *New England Journal of Medicine*.
- [5] Martcheva, M. (2015). *An introduction to mathematical epidemiology*, volume 61. Springer.
- [6] Smith, H. L. (1996). Monotone dynamical systems: an introduction to the theory of competitive and cooperative systems. *Bulletin (New Series) of the American Mathematical Society*, 33:203–209.
- [7] Team, E. E. et al. (2020). Note from the editors: World health organization declares novel coronavirus (2019-ncov) sixth public health emergency of international concern. *Eurosurveillance*, 25(5).

- [8] Wu, A., Peng, Y., Huang, B., Ding, X., Wang, X., Niu, P., Meng, J., Zhu, Z., Zhang, Z., Wang, J., et al. (2020). Genome composition and divergence of the novel coronavirus (2019-ncov) originating in china. *Cell Host & Microbe*.
- [9] Yeo, C., Kaushal, S., and Yeo, D. (2020). Enteric involvement of coronaviruses: is faecal–oral transmission of sars-cov-2 possible? *The Lancet Gastroenterology & Hepatology*.
- [10] Zhou, P., Yang, X.-L., Wang, X.-G., Hu, B., Zhang, L., Zhang, W., Si, H.-R., Zhu, Y., Li, B., Huang, C.-L., et al. (2020). Discovery of a novel coronavirus associated with the recent pneumonia outbreak in humans and its potential bat origin. *BioRxiv*.
- [11] Zhu, N., Zhang, D., Wang, W., Li, X., Yang, B., Song, J., Zhao, X., Huang, B., Shi, W., Lu, R., et al. (2020). A novel coronavirus from patients with pneumonia in china, 2019. *New England Journal of Medicine*.